Supporting Information

Synergistic adsorption and photocatalytic degradation of perfluorooctanoic acid in aqueous solution by a regenerable biochar-titania nanotube composite

Yingjie Liu, Dongjiao Lin, Yang Yu, Fei Wang, Weizhao Yin, Ying Liu, Peilin Ye, Yanyan Gong*

Guangdong Key Laboratory of Environmental Pollution and Health, School of Environment and Climate, Jinan University, Guangzhou 511443, China

*Corresponding author. E-mail address: yanyangong@jnu.edu.cn (Y. Gong).

Section S1. Chemicals and reagents

All chemicals used in this study were in the analytical grade or higher. Wheat straw (1.6 – 2.0 mm) was acquired from a farm in Donghai, Jiangsu Province, China. PFOA was obtained from Sigma-Aldrich (St. Louis, MO, USA). Perfluoro-n-(1,2-$^{13}C_2$) (M2PFOA) was obtained from Wellington Laboratories Inc. (Guelph, Ontario, Canada). Methanol was purchased from Thermo Fisher Scientific (Waltham, USA). Nano-TiO_2 (P25, 20 nm), tert-butanol, and NaOH were purchased from Macklin (Shanghai, China). HCl was obtained from the Guangzhou Chemical Reagent Factory (Guangzhou, China). Ammonium acetate, KI, and ascorbic acid were purchased from Aladdin (Shanghai, China). Isopropyl alcohol was acquired from Guangdong Guanghua Technology Co., Ltd. (Guangzhou, China). 5,5-Dimethyl-1-pyrroline N-oxide (DMPO) was obtained from Cool Chemistry (Beijing, China). Sodium tetraethyl borate was obtained from Anpel (Shanghai, China). Dimethyl sulfoxide was obtained from Shanghai Acmec Biochemical Co., Ltd. (Shanghai, China).

Section S2. Preparation of TNTs@biochar

Biochar was synthesized following a previously reported approach [1]. In brief, the dry wheat straws were heated at 600 °C for 2 h under nitrogen flow at 100 mL/min, soaked in 1 mol/L HCl solution for 24 h, washed with ultrapure water till the pH reached neutral, and then oven-dried at 105 °C for 24 h. TNTs@biochar was prepared following a revised hydrothermal method [2]. 1.2 g of TiO_2 and 1.2 g of the biochar were dispersed in 67 mL of a 10 M NaOH solution. The mixture was magnetically stirred for 12 h, transferred into an autoclave, and heated at 130 °C for 72 h. Upon gravity settling, the precipitate was collected and washed with ultrapure water until

the pH reached neutral and then oven-dried at 105 °C for 24 h. The dried particles were then calcined at 550 °C for 3 h at a nitrogen flow of 100 mL/min in a tube furnace to obtain the TNTs@biochar composite.

To test the effect of the supporting material, the composite was prepared with the addition of biochar and biomass (dry wheat straws), respectively (denoted as TNTs@biochar and TNTs@biomass). To test the effect of the biochar:TiO_2 mass ratio, the composite was synthesized at five biochar:TiO_2 mass ratios, namely, 0:1, 1:2, 1:1, 2:1, and 1:0. To test the impact of the calcination temperature, the composite was calcined at 250, 350, 450, and 550 °C with a biochar:TiO_2 mass ratio of 1:1. To determine the effects of the supporting material, the biochar:TiO_2 mass ratio, and calcination temperature on PFOA adsorption, PFOA adsorption tests were conducted with these TNTs@biochar composites following the procedure as described in Section 2.3 with a fixed reaction time of 24 h. To determine the effects on photodegradation of TNTs@biochar-adsorbed PFOA, the degradation tests were carried out following the procedure as described in section 2.4.

Section S3. Characterization of TNTs@biochar composite

The surface morphology of TNTs@biochar, biochar, and TNTs was conducted by scanning electron microscope (SEM) (Sigma500, Zeiss Corp., Jena, Germany). Transmission electron microscopy (TEM) was analyzed via a JEM 2100 Electron microscope (JEOL, Tokyo, Japan). The surface topographical feature was explored via an atomic force microscopy (AFM) (Bruker Dimension Icon, Germany). The specific surface area, pore size, and pore volume were obtained following the multipoint nitrogen adsorption-desorption approach using a physisorption analyzer (Autosorb iQ Station 1, Quantachrome Corp., Boynton Beach, Florida, USA). The surface functional groups of TNTs@biochar before and after PFOA adsorption were

analyzed by Fourier transform infrared spectroscopy (FTIR) (IRAffinity-1S, Shimadzu Corporation Inc., Kyoto, Japan). The crystalline compositions were detected by X-ray diffractometer (XRD) (D2 PHASER, Bruker, Germany). The UV-vis diffuse reflectance spectra (UV-vis DRS) were recorded on a UV-vis spectrophotometer (UV-2700, Shimadzu, Tokyo, Japan). The photoluminescence (PL) spectra were recorded using a Thermo Scientific Lumina fluorescence spectrophotometer (Thermo Fisher Scientific, MA, USA). The electrochemical properties were performed using an electrochemical workstation (CHI660E, Shanghai Chenhua Instrument Co., Shanghai, China). Cyclic voltammetry (CV) was carried out at a scan rate of 50 mV/s within a potential window of −0.1 to 0 V. Electrochemical impedance spectroscopy (EIS) was analyzed with a frequency range from 0.01 Hz to 100 kHz.

Section S4. Electron spin resonance assay

Electron spin resonance (ESR) assay was carried out to confirm the production of •OH and $•O_2^-$. To obtain the stage of quick •OH and $•O_2^-$ production, 10 g/L TNTs@biochar was subjected to UV irradiation at a wavelength of 254 nm and an intensity of 30.0 mW/cm^2 for 1 h in water and in DMSO solution, respectively [3]. 10 mL sample was withdrawn and mixed immediately with 100 μL DMPO to form DMPO–•OH and DMPO–$•O_2^-$ adducts, respectively. The mixtures were shaken for 5 min and analyzed using an ESR spectrometer (A300–10/12, Bruker, Karlsruhe, Germany).

Section S5. Toxicity prediction

The acute and chronic toxicities of PFOA and its photodegradation products to green algae, daphnid, and fish were predicted using the USEPA ECOSAR v1.11 software. For the acute toxicity data, the half-effective concentration for green algae

(EC_{50}, 96 h) and half-lethal concentrations for daphnid (LC_{50}, 48 h) and fish (LC_{50}, 96 h) were applied as the ecotoxicological endpoints. Chronic toxicity data (Chronic value, ChV) was estimated as the predicted geometric mean of the lowest observed effect level (LOEC) and no observed effect level (NOEC).

Section S6. Analytical methods

PFOA and M2PFOA were analyzed using an ultra-high-performance liquid chromatography system (UHPLC, Shimadzu Corporation Inc., Kyoto, Japan) equipped with an AB-Sciex 5500 triple quadrupole mass spectrometry system (Applied Biosystems, Foster City, CA, USA). 1 μL of the sample was injected into a Waters XBridge BEH C18 column (3 mm × 100 mm, 2.5 μm). A gradient mobile phase of ultrapure water and 4 mmol/L ammonium acetate in methanol were applied as the mobile phase at a flow rate of 300 μL/min. The mobile phase gradient expressed as the ratio of methanol to total solution was as follows: 0 – 1.0 min, 20%; 1.0 – 2.5 min, a linear increase from 20% to 95%; 2.5 – 6.0 min, 95%; 6.0 – 6.5 min, a linear decrease from 95% to 20%; and 6.5 – 8.5 min, 20%. The column temperature was 40 °C. The total run time of each injection was 8.5 min. Mass spectra data were collected in a negative electrospray ionization mode and chromatograms were recorded by a multiple reaction monitoring (MRM) mode. The compounds monitoring transition were 413, 369 m/z^+ for PFOA and 415, 370 m/z^+ for M2PFOA. The detection limits of PFOA and M2PFOA were 100 ng/L and 0.3 ng/L, respectively. The photodegradation byproducts were analyzed using a similar method except that the mobile phase gradient was as follows: 0 – 1.0 min, 20%; 1.0 – 6.0 min, a linear increase from 20% to 95%; 6.0 – 8.5 min, 95%; 8.5 – 10.0 min, a linear decrease from 95% to 20%; and 10.0 – 12.0 min, 20%. The total run time of each injection was 12.0

min. The compounds monitoring transition were 363, 319 m/z$^+$ for PFHpA, 313, 269 m/z$^+$ for PFHxA, 263, 219 m/z$^+$ for PFPeA, and 213, 169 m/z$^+$ for PFBA.

Section S7. Adsorption kinetics models

The pseudo-first-order (**Eq. (S1)**), pseudo-second-order (**Eq. (S2)**) [4], external mass transfer (**Eq. (S3)**) [5], and intraparticle diffusion models (**Eq. (S4)**) [6] were applied to interpret the data:

Pseudo-first-order model: $\mathrm{In}(q_e - q_t) = \mathrm{In}q_e - K_1 t$ (S1)

Pseudo-second-order model: $\frac{t}{q_t} = \frac{1}{K_2 q_e^2} + \frac{t}{q_e}$ (S2)

External mass transfer model: $\frac{-\mathrm{d}C}{\mathrm{d}t} = k_f a(C - C_s)$ (S3)

Intraparticle diffusion model: $q_e = k_i t^{0.5} + I$ (S4)

where q_t and q_e (μg/g) represent the adsorption capacity at t (h) and equilibrium, respectively, K_1 (h^{-1}) is the pseudo-first-order adsorption rate constant, K_2 (g/(μg·h)) is the pseudo-second-order adsorption rate constant, C and C_s are the concentrations of PFOA in bulk solution and at the interface, respectively (μg/L), k_f is the mass transfer coefficient (cm/s), a (m^2/m^3) is the specific area available for mass transfer per unit volume of the contactor; k_i is the intraparticle diffusion rate constant (μg/(g·h$^{0.5}$)), and I (μg/g) is the intercept related to the thickness of the boundary layer.

For the external mass transfer models, assume the PFOA sorption fits Langmuir isotherm (**Eq. (S5)**):

$$q_e = \frac{q_m k C_S}{1 + C_S} \quad \text{(S5)}$$

where k is the sorption equilibrium coefficient; and q_m (μg/g) is the maximum sorption capacity. q_e (μg/g) can be calculated by the following **Eq. (S6)**:

$$q_e = \frac{V}{m}(C_0 - C_s) \quad \text{(S6)}$$

Where V (L) is the contactor volume, m (g) is the mass of TNTs@biochar, and C_0 (μg/L) is the initial PFOA concentration in bulk solution. Combine **Eq. (S3)**, **(S5)**, and **(S6)** yielding **Eq. (S7)**:

$$-\frac{dc}{dt} = k_f a[C - \frac{1}{2}(\sqrt{(\frac{q_m m}{V} - C_0 + \frac{1}{k})^2 + \frac{4C_0}{k}}) - \frac{q_m m}{V} + C_0 - \frac{1}{k})] \quad \text{(S7)}$$

To describe the sorption data with the model, the concentration of PFOA in the bulk solution (C) is derived as a function of time (t) with **Eq. (S8)**:

$$C = b\exp[-ht] + C_0 - b \quad \text{(S8)}$$

where h (1/h) and b (μg/L) are the fitting parameters of the external mass transfer model, respectively. $h = k_f a$ and $b = C_0 - \frac{1}{2}(\sqrt{(\frac{q_m m}{V} - C_0 + \frac{1}{k})^2 + \frac{4C_0}{k}}) - \frac{q_m m}{V} + C_0 - \frac{1}{k})$ **Eq. (S8)** is applied to fit the experimental results with h and b as fitting parameters.

Section S8. Adsorption isotherm models

The classical Langmuir (**Eq. (S9)**), Freundlich (**Eq. (S10)**) [7], and dual-mode (**Eq. (S11)**) [8] models are employed to fit the adsorption isotherm data:

Langmuir model: $$q_e = \frac{q_m K_L C_e}{1 + K_L C_e} \quad \text{(S9)}$$

Freundlich model: $$q_e = K_F C_e^{\frac{1}{n}} \quad \text{(S10)}$$

Dual-mode model: $$q_e = K_d C_e + \frac{b q_m C_e}{1 + b C_e} \quad \text{(S11)}$$

where q_e (mg/g) stands for the equilibrium PFOA uptake, C_e (mg/L) represents the equilibrium PFOA concentration in the solution, K_L (mg/L) is the Langmuir sorption constant, q_m (mg/g) is the maximum Langmuir adsorption capacity of TNTs@biochar; K_F[(mg/g)/(mg/L)^n] is the Freundlich affinity coefficient, n is the exponential coefficient, K_d (L/mg) represents the linear distribution coefficient, and b (L/mg) is the Langmuir affinity constant.

Section S9. Photodegradation kinetic models

The pseudo-first-order (**Eq. (S12)**) and retarded first-order kinetic models (**Eq. (S13)**) were applied to simulate the PFOA degradation rate data:

Pseudo-first-order kinetic model: $$\ln\left(\frac{M_t}{M_0}\right) = -K_P t \quad \text{(S12)}$$

Retarded first-order kinetic model: $$\frac{M_0}{M_t} = \frac{1}{(1 + \alpha t)^{-K_\alpha/\alpha}} \quad \text{(S13)}$$

where M_0 (g) and M_t (g) are the mass of PFOA at time 0 and t h, respectively, K_p (h^{-1}) is the first-order rate constant, K_α (h^{-1}) is the retarded first-order rate constant, and α is the retardation factor indicating the degree of deviation from pseudo-first-order behavior [9].

Table S1. Elemental compositions of raw biochar, biochar, TNTs, and TNTs@biochar based on the EDS analysis.

Materials	Element weight percentage (wt.%)				
	C	O	Na	Ti	Total
Raw biochar	51.92	47.67	0.25	0.16	100.00
Biochar	89.26	8.95	1.11	0.69	
TNTs	4.00	37.59	4.39	54.01	
TNTs@biochar	62.35	13.64	0.64	23.37	

Table S2. BET surface areas, average pore diameter, and average pore volume of biochar, TNTs, and TNTs@biochar with various biochar:TiO_2 mass ratios.

	Biochar	TNTs@biochar with various biochar:TiO_2 mass ratios			TNTs
		Biochar:TiO_2=2:1	Biochar:TiO_2=1:1	Biochar:TiO_2=1:2	
BET surface area (m^2/g)	295.18	339.90	298.32	141.52	63.00
Average pore diameter (nm)	4.116	2.769	0.785	2.769	1.766
Average pore volume (cm^3/g)	0.304	0.374	0.307	0.176	0.086

Table S3. Pseudo-first-order, pseudo-second-order, external mass transfer, and intraparticle diffusion models applied for simulating PFOA adsorption kinetic by TNTs@biochar and the corresponding fitting parameters (Errors given as standard deviation).

Adsorption kinetic models	**Parameters**			
Pseudo-first-order	K_1 (h^{-1})	q_e (μg/g)		R^2
	0.453±0.099	196.152±47.517		0.807
Pseudo-second-order	K_2 (g/(μg·h))	q_e (μg/g)		R^2
	0.018±0.008	250.575±16.974		0.989
External mass transfer	k_f (cm/s)	h (1/h)	b (μg/L)	R^2
	$3.02\times10^{-4}\pm0.75\times10^{-4}$	2.307±0.403	69.853±3.508	0.972
Intraparticle diffusion	First stage (0–0.5 h)	k_i (μg/(g·$h^{0.5}$))	I (μg/g)	R^2
		215.805±48.228	0	0.926
	Second stage (0.5–4.0 h)	k_i (μg/(g·$h^{0.5}$))	I (μg/g)	R^2
		49.062±11.043	137.839±15.121	0.908

Note: q_e (μg/g) is PFOA uptake at equilibrium time; K_1 (h^{-1}) is the rate constant of the pseudo-first-order sorption; K_2 (g/(μg·h)) is the pseudo-second-order sorption rate constant; k_f (cm/s) is the mass transfer coefficient; h_1 (μg/(g·h)) represents the initial rate of the pseudo-first-order sorption; h_2 (μg/(g·h)) is the initial rate of the pseudo-second-order sorption; h (1/h) and b (μg/L) are the fitting parameters of the external mass transfer model, a (m^2/m^3) is the specific surface area available for mass transfer per unit volume of the contactor; k_i (μg/(g·$h^{0.5}$)) is the intraparticle diffusion rate constant, and I (μg/g) is the intercept related to the thickness of the boundary layer.

Table S4. Regression parameters of adsorption isotherm data of PFOA onto TNTs@biochar by Langmuir, Freundlich, and dual-mode isotherm models (Errors given as standard deviation).

Adsorption isotherm models	Parameters			
Langmuir	q_m (mg/g)	K_L (mg/L)		R^2
	1.257±0.141	3.820±1.375		0.916
Freundlich	K_F (mg/g)/(mg/L)^n	$1/n$		R^2
	0.973±0.025	0.368±0.035		0.983
Dual-mode	q_m (mg/g)	b (L/mg)	K_d	R^2
	0.480±0.048	80.619±32.143	0.457±0.050	0.978

Note: where q_e (mg/g) is the equilibrium PFOA uptake; K_L (mg/L) is the Langmuir sorption constant, q_m (mg/g) is the maximum Langmuir adsorption capacity of TNTs@biochar; K_F[(mg/g)/(mg/L)^n] is the Freundlich affinity coefficient, and n is the exponential coefficient; K_d (L/mg) is the linear distribution coefficient, b (L/mg) is the Langmuir affinity constant.

Table S5. Pseudo-first-order and retarded first-order kinetic models applied for simulating POFA degradation kinetics and the corresponding fitting parameters (Errors given as standard deviation).

Photodegradation kinetic models	Parameters		
Pseudo-first-order	K_P (h^{-1})		R^2
	0.071±0.003		0.984
Retarded first-order	K_α (h^{-1})	α (h^{-1})	R^2
	0.183±0.026	0.750±0.214	0.997

Note: where K_p (h^{-1}) is the first-order rate constant, K_α (h^{-1}) is the retarded first-order rate constant, and α is the retardation factor indicating the degree of deviation from pseudo-first-order behavior.

Table S6. PFOA and the detected degradation products during the photocatalytic degradation of pre-concentrated PFOA by TNTs@biochar.

Compounds	Perfluorooctanoic acid (PFOA)	Perfluoroheptanoic acid (PFHpA)	Perfluorohexanoic acid (PFHxA)	Perfluoropentanoic acid (PFPeA)	Perfluorobutanoic acid (PFBA)
Chemical formula	$C_7F_{15}COO^-$	$C_6F_{13}COO^-$	$C_5F_{11}COO^-$	$C_4F_9COO^-$	$C_3F_7COO^-$
Ion pairs (m/z^+)	413、369	363、319	313、269	263、219	213、169
Retention time (min)	4.3	7.1	6.72	6.19	5.21
CAS	335-67-1	375-85-9	307-24-4	2706-90-3	375-22-4

Table S7. Predicted acute and chronic toxicity levels of PFOA and the detected degradation products by ECOSAR program.

Compounds	Acute toxicity (mg/L)			Chronic toxicity (ChV) (mg/L)		
	Fish (LC_{50})/96 h	Daphnid (EC_{50})/48 h	Green algae (LC_{50})/96 h	Fish	Daphnid	Green algae
Perfluorooctanoic acid (PFOA)	10.10	7.44	16.22	1.34	1.50	7.58
Perfluoroheptanoic acid (PFHpA)	35.43	24.52	41.43	4.37	4.15	16.86
Perfluorohexanoic acid (PFHxA)	121.93	79.34	103.82	13.40	11.31	36.83
Perfluoropentanoic acid (PFPeA)	408.97	250.18	253.58	43.65	30.02	78.39
Perfluorobutanoic acid (PFBA)	408.94	250.18	253.58	43.65	30.02	78.39

Note: EC_{50} is half effective concentration, and LC_{50} is half lethal concentration.

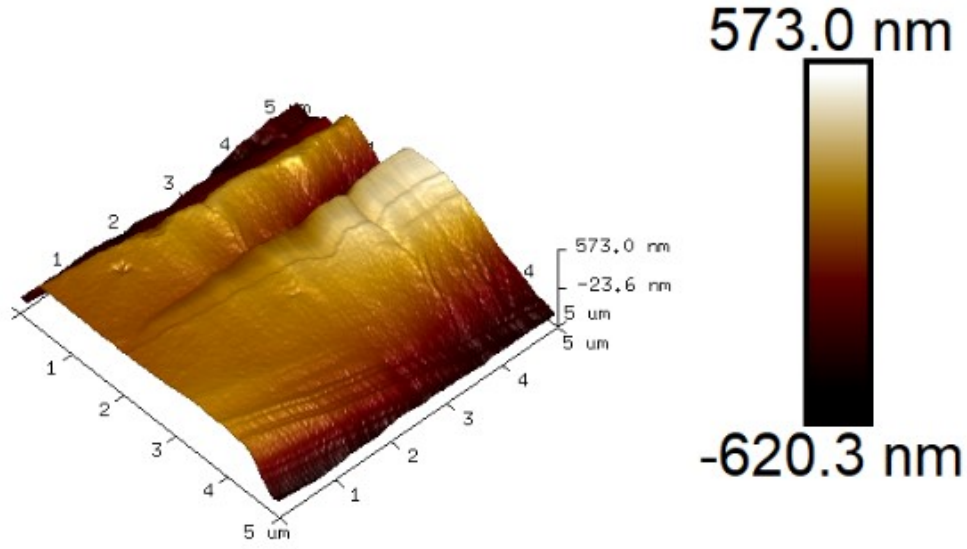

Fig. S1. AFM image of TNTs@biochar.

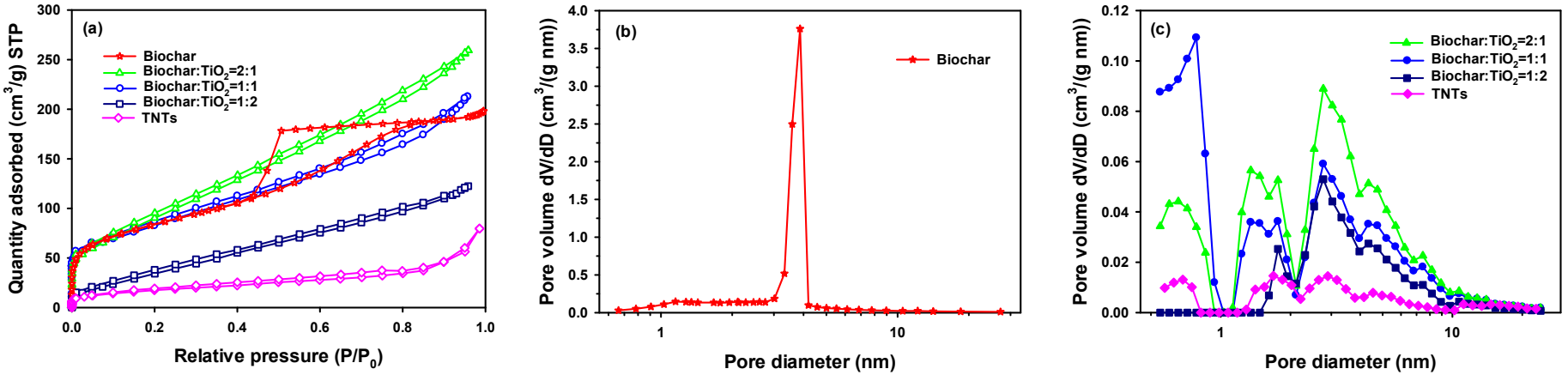

Fig. S2. (a) N_2 adsorption-desorption isotherms, and (b-c) pore size distributions of biochar, TNTs, and TNTs@biochar with various biochar:TiO_2 mass ratios. V represents pore volume, and D represents pore diameter.

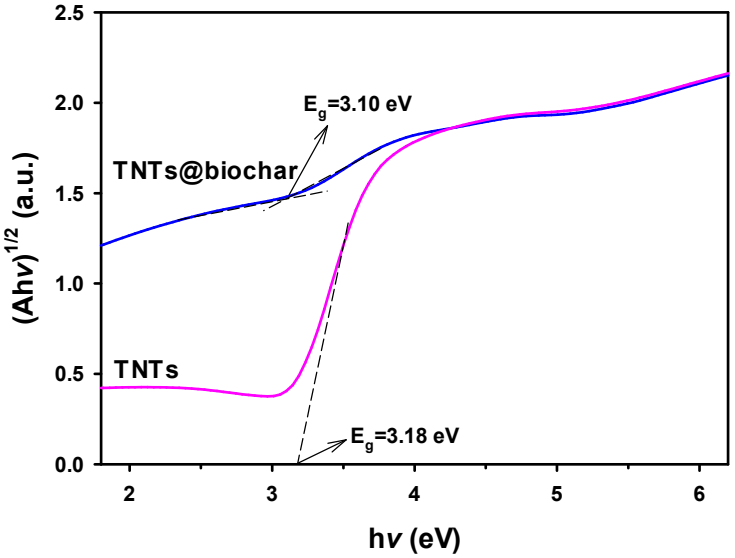

Fig. S3. Kubulka-Munk spectra of TNTs and TNTs@biochar.

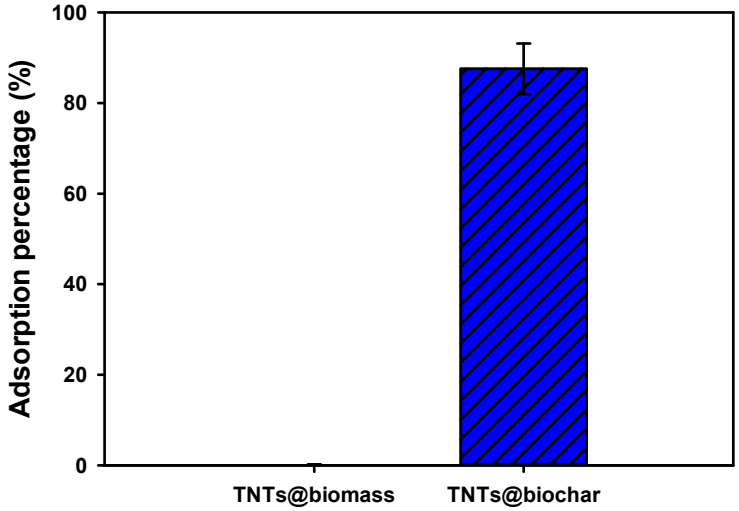

Fig. S4. Adsorption of PFOA in aqueous solution using TNTs@biomass and TNTs@biochar. Experimental conditions: initial PFOA = 100 μg/L, material dosage = 0.3 g/L, solution volume = 40 mL, reaction time = 24 h, pH = 7.0 ± 0.3, and temperature = 23 ± 2 °C.

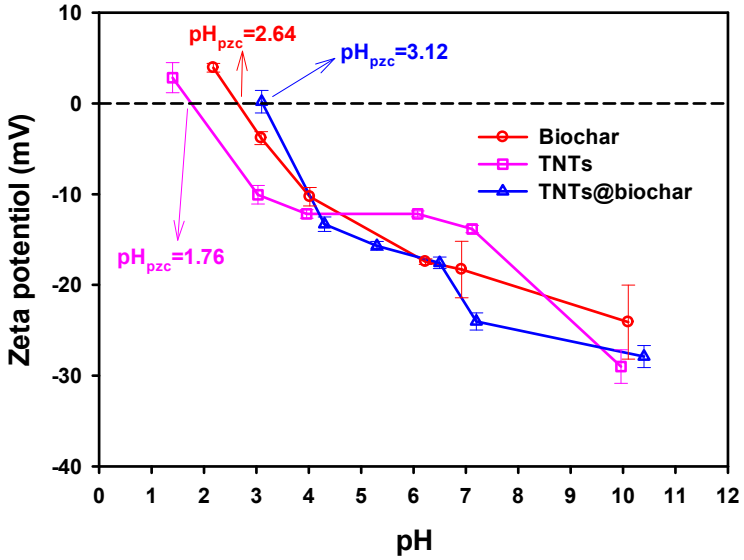

Fig. S5. Zeta potentials of biochar, TNTs, and TNTs@biochar at different pH values.

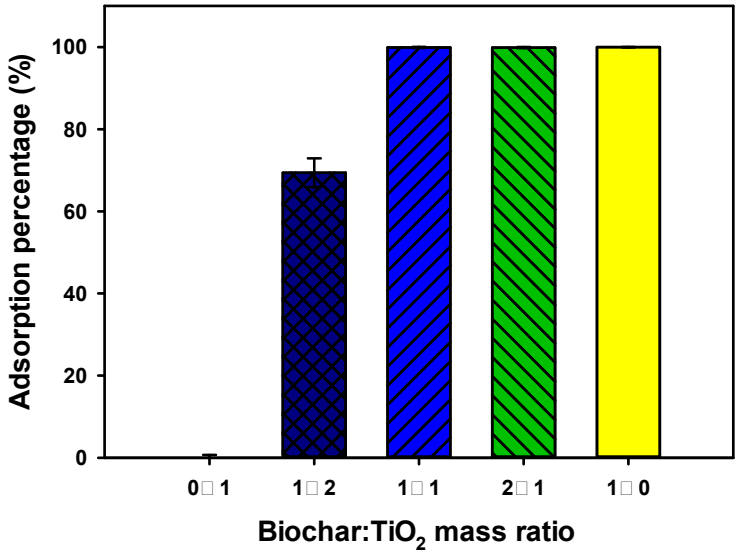

Fig. S6. Adsorption of PFOA by TNTs@biochar prepared at various biochar:TiO_2 mass ratio. Experimental conditions: initial PFOA = 100 μg/L, material dosage = 1.5 g/L, solution volume = 40 mL, reaction time = 24 h, pH = 7.0 ± 0.3, and temperature = 23 ± 2 °C.

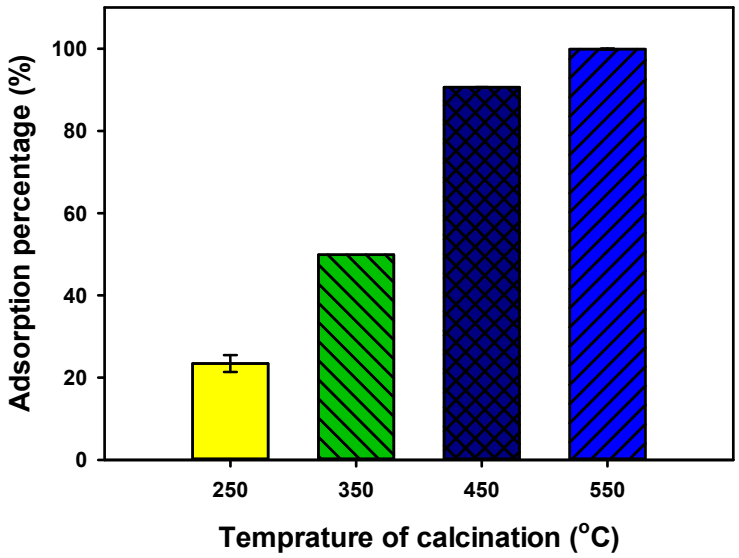

Fig. S7. PFOA adsorption via TNTs@biochar prepared at different calcination temperatures. Experimental conditions: initial PFOA = 100 μg/L, material dosage = 1.5 g/L, solution volume = 40 mL, reaction time = 24 h, pH = 7.0 ± 0.3, and temperature = 23 ± 2 °C.

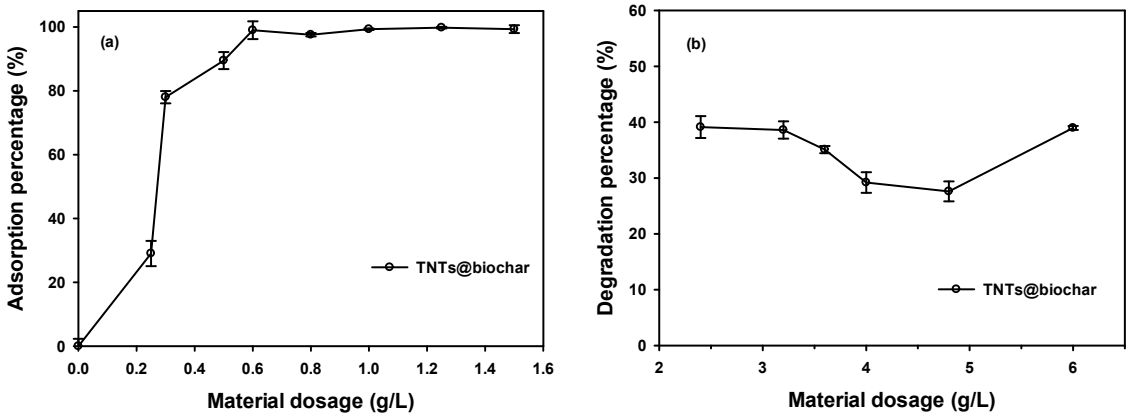

Fig. S8. (a) Effects of material dosage on adsorption of PFOA by TNTs@biochar. Experimental conditions: initial PFOA = 100 μg/L, material dosage = 0 – 1.5 g/L, solution volume = 40 mL, reaction time = 24 h, pH = 7.0 ± 0.3, and temperature = 23 ± 2 °C. (b) Effects of material dosage on photodegradation of pre-adsorbed PFOA by TNTs@biochar. Experimental conditions: initial pre-adsorbed PFOA quantity = 66.7 μg/g, material dosage = 2.4 – 6.0 g/L, solution volume = 10 mL, pH = 7.0 ± 0.3, temperature = 23 ± 2 °C, reaction time = 7 h, UV wavelength = 254 nm, and light intensity = 30.0 mW/cm^2.

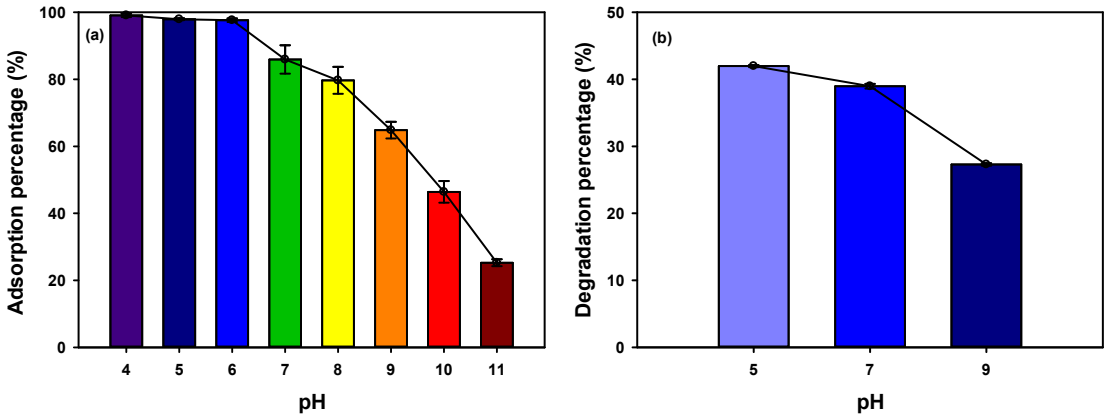

Fig. S9. (a) Effects of pH on adsorption of PFOA by TNTs@biochar. Experimental conditions: initial PFOA = 100 μg/L, material dosage = 0.3 g/L, solution volume = 40 mL, reaction time = 24 h, pH = 4.0 – 11.0, and temperature = 23 ± 2 °C. (b) Effects of pH on photodegradation of pre-adsorbed PFOA by TNTs@biochar. Experimental conditions: initial pre-adsorbed PFOA = 66.7 μg/g, material dosage = 6 g/L, solution volume = 10 mL, pH = 5.0, 7.0, and 9.0, temperature = 23 ± 2 °C, reaction time = 7 h, UV wavelength = 254 nm, and light intensity = 30.0 mW/cm^2.

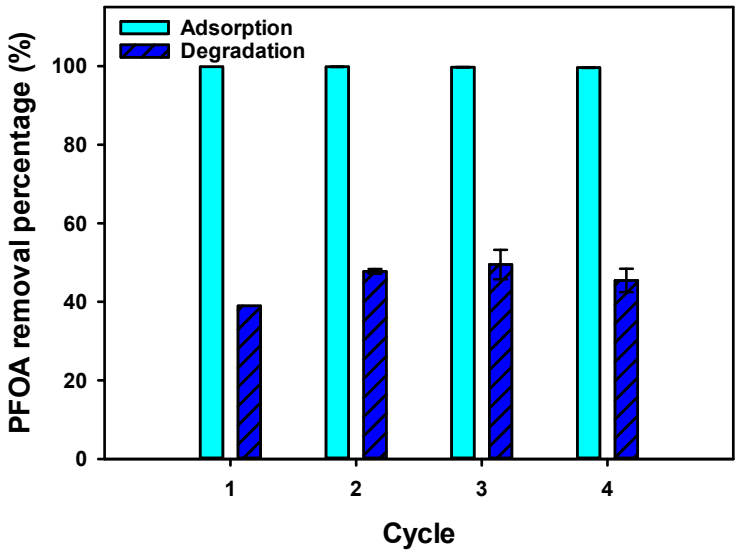

Fig. S10. Adsorption and photodegradation of PFOA in four consecutive cycles using the same TNTs@biochar. Experimental conditions: For each adsorption cycle, initial PFOA = 100 μg/L, material dosage = 1.5 g/L, solution volume = 40 mL, reaction time = 24 h, pH = 7.0 ± 0.3, and temperature = 23 ± 2 °C. For each photodegradation cycle, material dosage = 6.0 g/L, solution volume = 10 mL, pH = 7.0 ± 0.3, temperature = 23

± 2 °C, reaction time = 7 h, UV wavelength = 254 nm, and light intensity = 30.0 mW/cm^2.

References

1. H. Lyu, J. Tang, Y. Huang, L. Gai, E. Y. Zeng, K. Liber and Y. Gong, *Chem. Eng. J.*, 2017, **322**, 516-524.
2. F. Li, Z. Wei, K. He, L. Blaney, X. Cheng, T. Xu, W. Liu and D. Zhao, *Water Res.*, 2020, **185**, 116219.
3. P. Pieta, A. Petr, W. Kutner and L. Dunsch, *Electrochim. Acta*, 2008, **53**, 3412-3415.
4. Y.S. Ho and G. McKay, *Process Biochem.*, 1999, **34**, 451-465.
5. J. Luo, X. Luo, J. Crittenden, J. Qu, Y. Bai, Y. Peng and J. Li, *Environ. Sci. Technol.*, 2015, **49**, 11115-11124.
6. F. Wu, R. Tseng and R. Juang, *Chem. Eng. J.*, 2009, **153**, 1-8.
7. D. G. Kinniburgh, *Environ. Sci. Technol.*, 1986, **20**, 895-904.
8. W. R. Vieth and K. Sladek, *J. Colloid Sci.*, 1965, **20**, 1014-1033.
9. N. Watanabe, M. Takata, S. Takemine and K. Yamamoto, *Environ. Sci. Pollut. Res.*, 2018, **25**, 7200-7205.